optica

Nonlinear optics with full three-dimensional illumination: supplementary material

ROJIAR PENJWEINI[1,2], MARKUS WEBER[1,2], MARKUS SONDERMANN[1,2,*], ROBERT W. BOYD[3], AND GERD LEUCHS[1,2,3]

[1] Friedrich-Alexander-Universität Erlangen-Nürnberg (FAU), Department of Physics, Staudtstr. 7/B2, 91058 Erlangen, Germany
[2] Max Planck Institute for the Science of Light, Staudtstr. 2, 91058 Erlangen, Germany
[3] Department of Physics, University of Ottawa, 25 Templeton Street, Ottawa, Ontario K1N 6N5, Canada
[*] Corresponding author: markus.sondermann@fau.de

Published 11 July 2019

This document provides supplementary information to "Nonlinear optics with full three-dimensional illumination," https://doi.org/10.1364/OPTICA.6.000878. It gives detailed arguments for excluding four-wave mixing as the nonlinear process underlying the generation of frequency-tripled photons in our experiments. Furthermore, the methods and concepts used in the simulations are discussed.

1. INFLUENCE OF FOUR-WAVE MIXING AND KERR EFFECT

It is well known that third-harmonic generation (THG) by four-wave mixing (FWM) with light focused such that the beam waist lies in the middle of the interaction region is possible only if the phase mismatch, $\Delta k = 3k_1 - k_3$, is positive [1]. Here, k_1 is the wave number of the fundamental beam and k_3 is the wave number of the TH beam. In normal dispersive media (such as argon driven by 1064 nm light), with increasing frequency the refractive index increases and $\Delta k = \frac{6\pi}{\lambda_1}(n_1^{(0)} - n_3^{(0)})$ is negative, where λ_1 is the wavelength of the fundamental beam and $n_1^{(0)}$ and $n_3^{(0)}$ are the linear refractive indices for the fundamental beam and TH beam, respectively. Thus, THG by FWM is not possible in the normal dispersive media.

If THG is influenced by the Kerr effect, the phase mismatch will become a function of intensity and nonlinear refractive indices as

$$\Delta k_{\mathrm{Kerr}} = \frac{6\pi}{\lambda_1}[(n_1^{(0)} - n_3^{(0)}) + (n_1^{(2)} - n_3^{(2)})I], \tag{S1}$$

with $n_1^{(2)}$ and $n_3^{(2)}$ denoting the *nonlinear* refractive indices for fundamental and TH beam. I is the intensity of the fundamental beam. The nonlinear refractive index for a single intense fundamental beam with angular frequency ω is given by [1]

$$n_1^{(2)} = \frac{3}{4(n_1^{(0)})^2\epsilon_0 c_0}\chi^{(3)}(\omega = \omega + \omega - \omega), \tag{S2}$$

where ϵ_0 is the vacuum permittivity, c_0 is the speed of light in vacuum and $\chi^{(3)}$ is the third-order nonlinear susceptibility. The nonlinear refractive index for a weak frequency-tripled beam with angular frequency $\omega' = 3\omega$ in a medium influenced by an intense fundamental beam with angular frequency ω is [1]

$$n_3^{(2)} = \frac{3}{2(n_3^{(0)})^2\epsilon_0 c_0}\chi^{(3)}(\omega' = \omega' + \omega - \omega). \tag{S3}$$

Since the detuning of the pump as well as of the TH wave with respect to the lowest excited state of argon has the same sign, $\chi^{(3)}(\omega = \omega + \omega - \omega)$ and $\chi^{(3)}(\omega' = \omega' + \omega - \omega)$ have the same sign, too. Obviously, then the same holds true for $n_1^{(2)}$ and $n_3^{(2)}$. From Eq. (S2) and Eq. (S3) we conclude that

$$n_1^{(2)} - n_3^{(2)} = \frac{3}{4\epsilon_0 c_0}\left(\frac{\chi^{(3)}(\omega = \omega + \omega - \omega)}{(n_1^{(0)})^2} - \frac{2\chi^{(3)}(\omega' = \omega' + \omega - \omega)}{(n_3^{(0)})^2}\right). \tag{S4}$$

According to Eq. (S1), to get a positive Δk_{Kerr} and hence the possibility of THG for focused light, two conditions should be fulfilled. The first condition is

$$n_1^{(2)} - n_3^{(2)} > 0 \tag{S5}$$

and the second condition reads

$$|(n_1^{(2)} - n_3^{(2)})I| > |(n_1^{(0)} - n_3^{(0)})|. \tag{S6}$$

We cannot check the first condition quantitatively, because, to the best of our knowledge, the value of $\chi^{(3)}(\omega' = \omega' + \omega - \omega)$

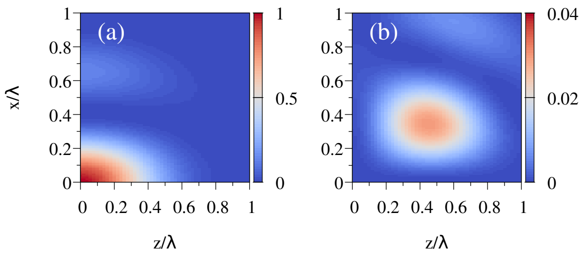

Fig. S1. Simulated intensity distributions in the focal region of a PM when focusing a radially polarized mode. The intensity of fields components polarized along the optical axis (z-axis) is shown in (a), the intensity of the field polarized in x-direction is depicted in (b). All intensity values are scaled by the maximum intensity in the focus. Both intensity distributions are symmetric with respect to the z-axis and the x-axis, respectively. The coordinates are given in units of the pump wavelength λ. The geometry of the PM is the same as for the one used in the experiment in the main text. Aberrations are not taken into account.

for a strong beam at 1064 nm and a weak beam at 355 nm has not been reported. If $\chi^{(3)}(\omega = \omega + \omega - \omega)$ is sufficiently smaller than $2\chi^{(3)}(\omega' = \omega' + \omega - \omega)$ such that the first condition is not fulfilled, then THG by FWM will not be possible. However, assuming that $\chi^{(3)}(\omega = \omega + \omega - \omega)$ is greater than $2\chi^{(3)}(\omega' = \omega' + \omega - \omega)$ and knowing that $n_3^{(0)} > n_1^{(0)}$, the first condition given by Eq. S5 is fulfilled. With this assumption, we check the second condition, setting $n_1^{(2)} - n_3^{(2)} \cong n_1^{(2)}$ which is the case at which the intensity I needed to achieve the condition given by Eq. S6 is minimum.

Considering the linear refractive indices of argon at 1064 nm and 355 nm [2], we calculate $n_1^{(0)} - n_3^{(0)} \cong -2.6 \times 10^{-5}$. For the fundamental beam at 1064 nm, the third-order nonlinear susceptibility of argon gas is $\chi^{(3)} = 7.8 \times 10^{-27}\,(\mathrm{m}^2/\mathrm{V}^2)/\mathrm{bar}$ [3]. The maximum intensity which we reach just before the breakdown threshold in argon gas is about $3.5 \times 10^{13}\,\mathrm{W/cm}^2$. Our experimental measurements are always done below the breakdown threshold. Setting I to the intensity at the breakdown threshold and using Eq. (S2) to calculate the nonlinear refractive index, we conclude that $|(n_1^{(2)} - n_3^{(2)})I| \cong |n_1^{(2)} I| = 7.7 \times 10^{-7}$ which is more than an order of magnitude smaller than $|(n_1^{(0)} - n_3^{(0)})|$. The difference would be even more pronounced when $n_1^{(2)} \approx n_3^{(2)}$, since then $|(n_1^{(2)} - n_3^{(2)})I|$ would be even smaller. Therefore, even assuming most favorable conditions Eq. S6 cannot be fulfilled. Thus we conclude that the generation of frequency-tripled photons in our experiment is not the result of THG by FWM, even when phase matching is influenced by the Kerr effect.

2. THEORETICAL CONSIDERATIONS

In what follows, we model the generation of frequency-tripled photons in the focus of a parabolic mirror.

The electric field of the incident focused beam induces a nonlinear polarization in the focal region of the parabolic mirror (PM). The contribution of the nonlinear polarization relevant for generating frequency-tripled photons is $\mathbf{P}_{3\omega}$. In the main text and above we have argued that six-wave mixing (SWM) is the responsible process for the generation of photons with frequency 3ω. In general, the 5$^{\text{th}}$-order susceptibility is a tensor. This provides the possibility for the mixing of field components with orthogonal states of polarization. In order for such a mixing to occur, correspondingly polarized fields have to be present [4]. As is evident from Fig. S1, field components with different states of polarization do occur in the focal region when focusing a radially polarized mode with a PM. The dominant field polarization is the one along the optical axis of the PM. However, the intensity of pump fields with orthogonal polarization is smaller by two orders of magnitude. Hence, the number of photons generated by cross coupling of longitudinal and transverse field components must be such low as well. In addition, this effect must be even more pronounced, since the dominant longitudinal components are localized close to the optical axis (confined within half a wavelength distance from the optical axis), whereas the transverse components have their maximum intensity off the optical axis (in a region where the longitudinal field is strongly suppressed), c.f. Fig. S1. Thus, any nonlinear signal polarized orthogonal to the optical axis can be estimated to be at maximum of order 10^{-3} of the maximum longitudinally polarized signal. The same reasoning applies for the generation of longitudinally polarized tripled-frequency photons from orthogonally polarized pump fields. We therefore approximate the 5$^{\text{th}}$-order susceptibility as a scalar $\chi^{(5)}$ and write the nonlinear polarization as

$$\begin{aligned}\mathbf{P}_{3\omega} &= \mathbf{P}^{(5)} \\ &= 5\epsilon_0\chi^{(5)}(3\omega = \omega+\omega+\omega+\omega-\omega)\mathbf{E}^4(\mathbf{r})\mathbf{E}^*(\mathbf{r}),\end{aligned} \tag{S7}$$

where the factor 5 is the degeneracy factor and $\mathbf{E}(\mathbf{r})$ is the electric field of the focused fundamental beam. $\mathbf{r} = 0$ is the position of the geometrical focus of the PM.

Because $\mathbf{P}_{3\omega}$ is a dipole-moment density, the dipole moment oscillating at 3ω that is induced in a volume element V_i is given by

$$\boldsymbol{\mu}_{3\omega,i} = \int_{V_i} \mathbf{P}_{3\omega} d^3\mathbf{r}\,. \tag{S8}$$

In our simulations we associate V_i with the volume of a unit cell of the simulation grid. The light emitted by each dipole is collected by the parabolic mirror and propagates towards the detector. The detected signal is given by the interference of all these fields, with the amplitude of the field emerging from V_i being proportional to $\mu_{3\omega,i}$. We anticipate this interference process by introducing an effective dipole moment

$$M_{3\omega} = \sum_i \gamma_i \cdot \mu_{3\omega,i} \tag{S9}$$

where the γ_i are real weighting factors that account for the projection onto a detection mode (see Sec. 3 for a discussion on the influence of the spatial separation of the dipole moments $\mu_{3\omega,i}$ onto the overall signal).

The total power that is radiated at frequency 3ω by the dipole moment $M_{3\omega}$ amounts to [5, Eq. 9.24]

$$W_{3\omega} = \frac{(3\omega)^4}{12\pi\epsilon_0 c_0^3}|M_{3\omega}|^2\,. \tag{S10}$$

The medium is excited with pulses of Gaussian envelope of FWHM τ. Accounting for the observed 5$^{\text{th}}$-order dependence of the THG photons on excitation power, the duration of the THG pulse is $\tau/\sqrt{5}$. Therefore, the number of frequency-tripled photons per pulse becomes

$$N_{3\omega} = \frac{W_{3\omega}\tau}{3\sqrt{5}\hbar\omega}\,, \tag{S11}$$

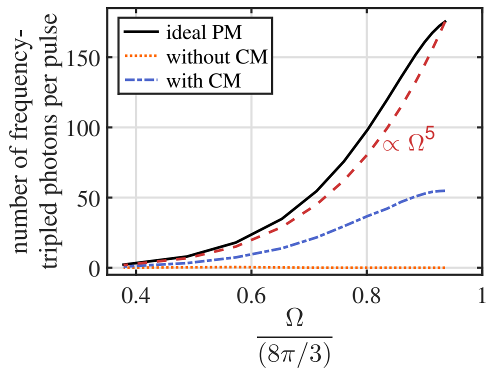

Fig. S2. Simulated frequency-tripled photon number vs solid angle used for focusing. The dotted line is for the case of using our PM without correcting for its aberrations. The dash-dotted line is for the case of employing a CM in our setup, which compensates the aberrations of our PM up to a Strehl ratio of 79%. The solid line is for the case of an ideal PM without any aberrations. The dashed line denotes a curve $\propto \Omega^5$ for comparison. The absolute values of frequency tripled photons per pulse were obtained by fitting the case 'with CM' to the experimental data.

where $3\hbar\omega$ is the energy of a frequency-tripled photon. Combining Eqs. (S8) to (S11) we arrive at

$$N_{3\omega} = \frac{225\epsilon_0\omega^3\tau\chi^{(5)^2}}{4\sqrt{5}\pi\hbar c_0^3}\left|\sum_i \gamma_i \int_{V_i} \mathbf{E}^4(\mathbf{r})\mathbf{E}^*(\mathbf{r})d^3\mathbf{r}\right|^2. \quad \text{(S12)}$$

The complex electric field $\mathbf{E}(\mathbf{r})$ in the focal region of the PM is calculated by using the Debye integral method [6]. Our numerical implementation of this method is explained in detail in Ref. [7]. By integrating over complex fields we explicitly account for the spatial variation of the phase of $\mathbf{P}_{3\omega}$. In our calculations we take into account the measured aberrations of our PM, the measured phase-front induced by the CM as well as the field distribution of the radially polarized doughnut mode. All aberrations are modeled as relative phases of the electric field distribution incident onto the PM. The pulse energy and duration are the same as in the experiment underlying Fig. 3 in the main text.

For the nonlinear susceptibility $\chi^{(5)}$ there is – to the best of our knowledge – no value reported in literature that was obtained in a comparable experimental setting, i.e. the generation of the TH of 1064 nm light by SWM. Ref. [3] reports $\chi^{(5)}$ for generating the fifth harmonic of 1064 nm light, whereas some $\chi^{(5)}$ values have been determined for SWM processes involving (deep) ultraviolet light, see Ref. [8] and references therein. Therefore, we here use $\chi^{(5)}$ as a fit parameter with which we quantitatively match the outcome of the simulations to the experimental results.

Fig. S2 shows the result of simulating the generation of frequency-tripled photons as a function of the solid angle used for focusing. We consider three cases, as shown in Fig S2.

In the first case, we model a PM without any aberrations, i.e. at the diffraction limit. The number of photons at frequency 3ω grows monotonically with increasing solid angle. This result can intuitively be understood from the fact that the focal intensity of the pump beam scales linearly with the solid angle Ω [9]. One would thus expect the conversion efficiency of an N-th order process to scale with solid angle as Ω^N. However, our simulation results do not show this Ω^5 dependence. We attribute this different result to the complicated spatial distribution of $\mathbf{E}(\mathbf{r})$ in the focal region: for increasing solid angle, the maximum intensity of the pump field in the focal region grows with Ω. However, the focal volume shrinks when increasing the solid angle (see simulations in Fig. S3). Also the spatial distribution of the phase of $\mathbf{E}(\mathbf{r})$ changes upon varying Ω. All these effects result in the behavior observed in the simulation.

As a second case, we model the PM used in the experiments without any aberration compensation, the number of generated frequency-tripled photons is very low at each investigated solid angle, cf. Fig. S2. The maximum of ~ 0.5 photons per pulse occurs at a solid angle of $\Omega = 0.57 \cdot 8\pi/3$. That is, the steady increase of the photon number for increasing Ω is no longer observed. The latter observation can be explained by the spatial distribution of the aberrations over the surface of the PM. Similar effects are also observed for other parabolic mirrors [10]. Such aberrations appear to be typical for deep parabolic mirrors, and seem to represent the current state of the art.

Finally, as a third case we calculate the number of frequency-tripled photons for the case of compensating the aberrations of the PM with a compensation mirror (CM) as described in the main text. This case is used to fit the simulations to the experimental results with $\chi^{(5)}$ as the only fit parameter. The simulation yields a steady increase of the photon number with increasing solid angle. Despite some saturation behavior at solid angle fractions beyond 90%, the results for the combination PM+CM shows *qualitative* similarities with the diffraction-limited case. However, the absolute photon numbers are considerably smaller than in the diffraction limited case. This latter observation is readily explained by the still non-optimum aberration compensation, which is expressed through a Strehl ratio of 79%. In the case of a nonlinear optical process as investigated here, the influence of a non-unit Strehl ratio should exponentiate to the order of the nonlinear process. For the largest solid angle used for focusing and for a fifth-order process, the simulation results approximately exhibit this behavior.

3. COLLECTING THIRD-HARMONIC SIGNALS FROM SPATIALLY SEPARATED DIPOLES

In typical nonlinear optics experiments the light generated in a wave-mixing process is collected from an extended spatial region. This necessitates the account of the relative phases of the electric fields generated at different positions when calculating the total power that is generated in the nonlinear process. There are two contributions to the relative phases. One stems from the relative phase of the local pump field, which determines the phase of the nonlinear polarization. This contribution is directly included in our simulations, cf. Eq. S12. The second contribution is determined by the optical path-length difference (OPD) from the different source dipoles in the nonlinear medium to the point of detection. We now discuss how to account for this contribution in our particular scenario.

Whereas the OPD is readily defined in an experiment in which the detection occurs only under a small solid angle, the situation is more complicated when collecting light over the full solid angle. For two sources separated by a distance d the OPD to a point of observation lying on a circle with radius $\gg d$ is given by

$$\mathrm{OPD} = d \cdot \cos\vartheta \quad \text{(S13)}$$

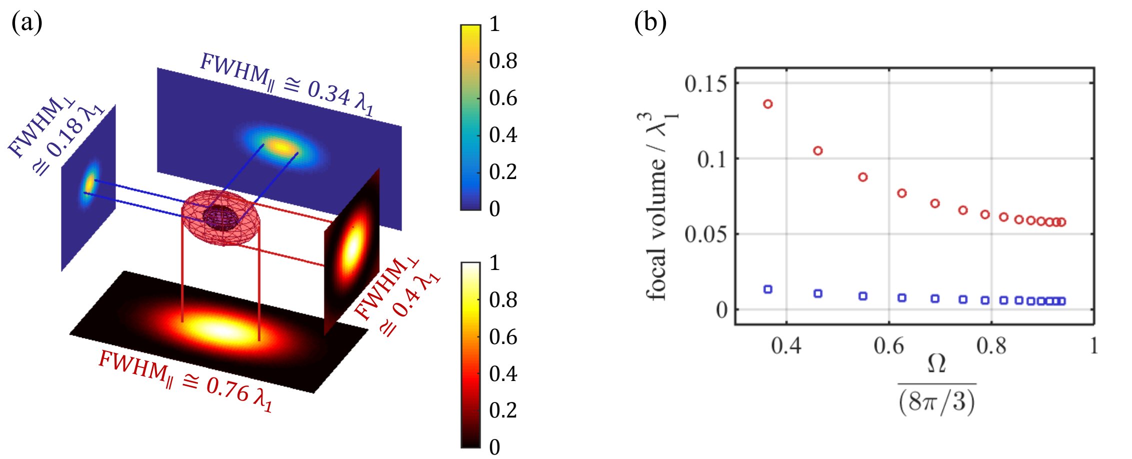

Fig. S3. (a) Simulated focal volume of the fundamental beam focused by the PM (outer spheroid) and the effective volume in which the frequency-tripled beam is generated through SWM (inner spheroid). Aberrations of the PM are corrected for by using the CM. To obtain the respective volumes the FWHMs of the corresponding intensity distributions are determined. Both intensity distributions are scaled to their respective maximum values. Bright color indicates high intensity. The effective volume of frequency-tripled photon generation is determined from the fifth power of the intensity distribution of the fundamental beam. The major axis of each spheroid equals the FWHM$_{||}$ of the corresponding distribution along the axis of the PM and the minor axis is the FWHM$_{\perp}$ of the distribution in the focal plane perpendicular to the axis of the PM. (b) Focal volume vs. solid angle: The red circles correspond to the focal volume of the fundamental beam focused by the PM. The blue squares correspond to the effective volume for frequency-tripled generation. All values are normalized to λ_1^3 where λ_1 is the wavelength of the fundamental beam.

with ϑ the angle to some reference direction. Thus, there is no unique OPD that is valid along all of the directions defined by the wave vectors of the dipolar emission of two separated sources. Moreover, the OPD is zero when averaging over ϑ.

However, when collecting light over the entire solid angle with a deep PM as in this work, the position of the light source determines the phase front of the mode that is reflected off the parabolic surface. These phase fronts can be expressed in terms of misalignment functionals, which in general have to be calculated numerically by ray tracing [11]. For the experimental scenario treated here, we can make some simplifying assumptions that lead to analytic expressions.

First, the focused pump field is predominantly polarized parallel to the optical axis of the PM. Thus the nonlinear polarization and consequently all induced dipole moments oscillating at 3ω are oriented along this direction. Since the extent of the focus is on the order of a wavelength or even smaller, we assume that the intensity distribution of the emission of all these dipoles is the same as the one for a dipole located at the geometric focus of the mirror. After collimation by the PM and ignoring an overall amplitude factor this intensity distribution reads [12]

$$I(r) \propto \frac{(r/f)^2}{[(r/f)^2/4+1]^4} \tag{S14}$$

with f the PM focal length and r the distance of a point in the aperture plane of the PM to the optical axis.

Second, the simulations of the focal intensity distribution of the pump light (cf. Sec. 2) reveal that the electric field $\mathbf{E}(\mathbf{r})$ is effectively concentrated in a narrow region along the optical axis of the PM. Since we observe that the generation of frequency-tripled photons is proportional to the fifth order of the pump power, we examine the distribution of $|\mathbf{E}(\mathbf{r})|^{10}$. We find that the half-width at half-maximum of this distribution in lateral direction is about $0.1\lambda_1$ for using the full mirror. In the axial direction the width is slightly larger. For somewhat smaller solid angles, as was the case in our measurements, the focal field distribution elongates along the optical axis while the lateral extent is practically constant. We therefore infer that the phase fronts of the TH light collected by the PM are mainly influenced by the axial position of the emitters and that phase front distortions due to lateral displacements can be neglected. Identifying ϑ in Eq. S13 with the emission angle of the dipole radiation pattern, the optical path-length difference of the emission from a dipole after collimation by the PM can be written as

$$\mathrm{OPD}_i(r) = z_i \, \frac{1-(r/2f)^2}{1+(r/2f)^2} \quad , \tag{S15}$$

where z_i is the axial displacement of the induced dipole $\mu_{3\omega,i}$ from the PM focus.

For calculating the interference of the fields emitted by all dipoles $\mu_{3\omega,i}$ in the focal region, we project each field distribution on a detection mode. We take the detection mode to be the field distribution that is emitted by the largest dipole moment. This dipole is located where the amplitude of the pump field is maximum, the corresponding axial coordinate is $z_{\max}$. Then, the overlap of the emission from dipole $\mu_{3\omega,i}$ with the detection mode reads

$$\gamma_i = \frac{\int I(r) \cdot \cos\left(\frac{6\pi}{\lambda_1}(z_i - z_{\max})\frac{1-(r/2f)^2}{1+(r/2f)^2}\right) r dr}{\int I(r) \, r dr} \quad , \tag{S16}$$

with the integration performed over the entire aperture of the PM. This is the factor γ_i employed in the calculation of the number of frequency-tripled photons in Eq. S12 in the main part.

REFERENCES

1. R. W. Boyd, *Nonlinear optics, 3rd* (Academic press, 2008).

2. M. N. Polyanskiy, "Refractive index database," https://refractiveindex.info (2018). [Accessed on 2018-08-23].
3. X. F. Li, A. L'Huillier, M. Ferray, L. A. Lompré, and G. Mainfray, "Multiple-harmonic generation in rare gases at high laser intensity," Phys. Rev. A **39**, 5751–5761 (1989).
4. G. Stegeman, D. G. Papazoglou, R. Boyd, and S. Tzortzakis, "Nonlinear birefringence due to non-resonant, higher-order kerr effect in isotropic media," Opt. Express **19**, 6387–6399 (2011).
5. J. D. Jackson, *Classical Electrodynamics* (Wiley, New York, 1999), 3rd ed.
6. B. Richards and E. Wolf, "Electromagnetic diffraction in optical systems. ii. structure of the image field in an aplanatic system," in *Proceedings of the Royal Society of London A,* , vol. 253 (The Royal Society, 1959), pp. 358–379.
7. N. Lindlein, M. Sondermann, R. Maiwald, H. Konermann, U. Peschel, and G. Leuchs, "Focusing light with a deep parabolic mirror," arXiv:1905.05997 [physics.optics] (2019).
8. J. Kutzner and H. Zacharias, "Vuv generation by frequency tripling the third harmonic of a picosecond khz nd: Ylf laser in xenon and mercury vapour," Appl. Phys. B: Lasers Opt. **66**, 571–577 (1998).
9. M. Sondermann, N. Lindlein, and G. Leuchs, "Maximizing the electric field strength in the foci of high numerical aperture optics," arXiv:0811.2098 [physics.optics] (2008).
10. L. Alber, M. Fischer, M. Bader, K. Mantel, M. Sondermann, and G. Leuchs, "Focusing characteristics of a 4π parabolic mirror light-matter interface," J. Eur. Opt. Soc. Publ. **13**, 14 (2017).
11. G. Leuchs, K. Mantel, A. Berger, H. Konermann, M. Sondermann, U. Peschel, N. Lindlein, and J. Schwider, "Interferometric null test of a deep parabolic reflector generating a hertzian dipole field," Appl. optics **47**, 5570–5584 (2008).
12. N. Lindlein, R. Maiwald, H. Konermann, M. Sondermann, U. Peschel, and G. Leuchs, "A new 4π-geometry optimized for focusing onto an atom with a dipole-like radiation pattern," Laser Phys. **17**, 927–934 (2007).